Performance Analysis of FSO Communication Over Atmospheric Turbulence and Pointing Error

Vinod Kiran Kappala*, Jayashree Pradhan#, Natasha Pawar#, Yamuna Tumma, Santos Kumar Das#
School of Electronics Engineering (SENSE), VIT-AP University, Amaravati, AP, India
#Department of Electronics and Communication Engineering
National Institute of Technology Rourkela, India
*Email: vinod.k@vitap.ac.in

***Abstract*—Free space optics (FSO) communication operates over the unlicensed spectrum providing high throughput, high security, and ease of installation. FSO can solve the last mile problem of connectivity with wide applications, i.e., disaster recovery, campus connectivity, backhaul connection, etc. However, the deployment scenario is constrained due to the severe atmospheric conditions and a precise line of sight requirements. This research work analyzes the performance of FSO communication under the combined effect of pointing errors (PEs) and atmospheric turbulence. The effects of jitter and boresight for PEs are modelled with generalized Nakagami-m distribution. A closed-form average bit error rate (BER) is derived for the generalized phenomenon and the theoretical results are compared with simulation and experimental results. Also, an experimental testbed is designed and implemented under a controlled indoor environment to analyze the atmospheric turbulence affects on FSO communication.**

***Index Terms*—Atmospheric turbulence, BER, Experimental testbed, FSO.**

I. Introduction

Free space optics (FSO) is a high-speed technology only for line-of-sight (LOS), which establishes point-to-point communication. Over unlicensed bandwidth, FSO provides high data rates, with low power consumption, less cost, and high security [1]. FSO communication links are effective for rates of 1-10 Gb/s with operational link distances up to several kms. Due to these desirable characteristics, FSO finds importance in wide applications such as remote sensing, disaster recovery, radio astronomy, campus connectivity, outdoor wireless access, metropolitan area network, fiber backup and last-mile access connectivity [2].

Apart from the advantages, various environmental conditions restrict FSO communication in practice. Aerosol scattering (i.e., snow, rain and fog), wind-induced building sway, thermal expansion, and earthquakes degrade the overall system performance. Additionally, in clear weather, the efficacy is affected for FSO transmission caused by scintillation created by turbulence i.e., change in temperature across the atmosphere creates the turbulent environment [3]. The temperature fluctuations create different refractive index with the signal's path, resulting in fading at the receiver [4]. Several mathematical models have been discussed to account for this variability from strong to weak fading environments [5], [6]. Low seismic waves, building sway, vibrations, and thermal expansions create pointing errors (PEs), which causes transmitter-receiver misalignment resulting in the FSO link failure. PEs include boresight, caused due to prescribed displacement from the receiver, and jitter, which is caused by random changes in the beam [7].

The effect of turbulence due to air and PEs are combined and investigated in the literature [8]–[15]. In [8], the authors investigated the pre-amplified FSO system performance for non-return-to-zero-on-off keying (NRZ-OOK) and an amplified spontaneous emission (ASE) noise over M-distributed turbulence due to atmosphere and Rayleigh distribution of PEs. In [9], the authors investigated the statistical model for combined channel weak and moderate turbulence regimes using log-normal and Gamma-Gamma distribution. While, PEs are modelled using Rician distribution, which corresponds to the non-zero boresight effect. In [10], the BER performance of FSO communication due to PEs modelled as Rayleigh distributions correspond to identical jitters. Atmospheric turbulence is modelled as a $K-$distribution. In [11], the authors investigated attenuation due to the atmosphere, which is caused by different conditions of weather and the fading-like environment caused due to turbulence. The performance of error detection using intensity-modulated direct detection (IM/DD) is assessed. In [12], [13], the authors analyzed the BER of FSO system under atmospheric turbulence and PEs.Atmospheric turbulence with moderate to strong regime is modelled with Gamma-Gamma distribution and PEs as Rayleigh distribution. In [14], the authors evaluated average bit error rate for atmospheric turbulence with Gamma-Gamma distribution and Hoyt distribution for PE where the unequal jitter variance in either direction (horizontal and vertical) is considered. In [15], the authors analyzed the outage analysis of FSO communication considering PEs with Rayleigh distribution for jitter and Rician for non-zero boresight error effects. Most research considers the PEs effect individually, i.e., jitter or a boresight error. In [16], the authors analyzed the performance considering PEs modelled as Nakagami-m distribution which can include the different effects of PEs on the suitable selection of parameters.

This research paper analyses BER's closed-form expression under combined atmospheric turbulence and PEs. In addition, an experimental testbed has been developed and implemented to analyze FSO communication system performance under various channel regimes.

The remaining part of the paper is structured as follows: Section II, discusses the adopted system model adopted. Section III, presents the mathematical framework of the statistical channel and the closed-form average BER. Section IV discusses the experimental testbed design and measurements. Section V analyses the numerical and experimental results and finally, Section VI concludes the research work.

979-8-3503-0219-6/23/$31.00 ©2023 IEEE

II. System Model

Consider an FSO communication system with IM/DD operating in the presence of scintillation due to atmospheric turbulence and PEs. Direct detection with a photodetector at the receiver converts optical power into an electrical signal. At the receiver, the received signal y is denoted as

$$y = hx + n, \tag{1}$$

where h represents the free space channel, transmitted signal with ON/OFF keying (OOK) modulation, x has power 0 or $2P_t$, P_t is the average transmitted optical power. n represents the Additive white Gaussian noise (AWGN), due to the thermal/shot noise (i.e., zero mean and variance, σ_n^2). The receiver's instantaneous signal-to-noise ratio (SNR) for a slow fading channel with OOK signalling can be represented as,

$$SNR\left(h\right) = \frac{2\,P_t^2\,R^2\,h^2}{\sigma_n^2}, \tag{2}$$

where, R represents the detector responsivity considered as unity, and $SNR(h)$ is random due to the influence of h. The average SNR defined as [17],

$$\overline{SNR\left(h\right)} = \frac{2\,P_t^2\,R^2\,E\left[h^2\right]}{\sigma_n^2}, \tag{3}$$

where, $E\left[h^2\right]$ is a channel variance with zero mean. The overall random variations of the channel, h, caused by PE (h_p), atmospheric turbulence (h_a), and path loss component (h_l). In this case, h_a and h_p are random, while h_l is deterministic. The combined channel condition can be expressed by as [9],

$$h = h_a\,h_p\,h_l. \tag{4}$$

The detailed modelling of the channel caused by random variations of atmospheric turbulence and PEs can be explicitly represented as follows:

A. Atmospheric Turbulence

Atmospheric turbulence created due to variations in the temperature of the atmosphere creates random intensity and phase fluctuations in the received signal. A moderate to strong turbulence regime can be represented using the Gamma-Gamma probability density function (PDF) expressed as [18],

$$f_{h_a}\left(h_a\right) = \frac{2\left(\alpha_l\beta_s\right)^{\frac{\alpha_l+\beta_s}{2}}}{\Gamma\left(\alpha_l\right)\Gamma\left(\beta_s\right)} h_a^{\frac{\alpha_l+\beta_s}{2}-1} K_{\alpha_l-\beta_s}\left(2\sqrt{\alpha_l\beta_s h_a}\right), \tag{5}$$

where, α_l, β_s represent the large-scale and small-scale eddies in the turbulent environment respectively. $K_\vartheta(.)$ is the modified Bessel function of second kind and order ϑ. Under a plane wave propagation, α_l, β_s can be represented as [19],

$$\alpha_l = \left(\exp\left(\frac{0.49D_0^2}{\left(1+0.56D_0^{\frac{12}{5}}\right)^{\frac{7}{6}}}\right)-1\right)^{-1} \tag{6}$$

$$\beta_s = \left(\exp\left(\frac{0.51D_0^2}{\left(1+0.69D_0^{\frac{12}{5}}\right)^{\frac{5}{6}}}\right)-1\right)^{-1}, \tag{7}$$

where, D_0^2 represents the plane wave's Rytov variance, whose value is determined by the atmospheric turbulence's refractive index expressed as,

$$D_0^2 = 1.23\,C_n^2\,k^{\frac{7}{6}}\,z^{\frac{11}{6}}, \tag{8}$$

where, C_n^2 represents the refractive index parameter determining the strength of turbulence, optical number $k = \frac{2\pi}{\lambda}$ and λ is the operating wavelength for FSO system.

Equation (5) using Meijer-G [20] can also be represented as shown below,

$$f_{h_a}\left(h_a\right) = \frac{\left(\alpha_l\beta_s\right)^b}{\Gamma\left(\alpha_l\right)\Gamma\left(\beta_s\right)}\,h_a^{(b-1)} \\ G_{0,2}^{2,0}\left(\begin{matrix}-\\ \frac{\alpha_l-\beta_s}{2},\frac{\beta_s-\alpha_l}{2}\end{matrix}\;\middle|\;\alpha_l\beta_s h_a\right), \tag{9}$$

where $b = \frac{\alpha_l+\beta_s}{2}$ and $G_{p,q}^{m,n}$ is the Meijer-G function.

B. Pointing Error Model

Pointing errors in the FSO system present a significant challenge in the evaluation of reliability and performance [12]. A Gaussian beam from the transmitter propagating through the free space, with the received power can be represented as [2],

$$h_p\left(r;z\right) \approx A_o\,\exp\left(\frac{-2r^2}{w_{zeq}^2}\right), 0 \le h_p \le A_o \tag{10}$$

where z represents the operational link distance and r represents the beam radial displacement from the detector center. w_{zeq} is the equivalent beam width defined as $w_{zeq} = \sqrt{\sqrt{\pi}\,erf\left(\nu\right)\,w_z^2/2\nu e^{-\nu^2}}$, maximum power received when radial displacement at r = 0 is given as, $A_0 = \left[erf\left(\nu\right)\right]^2$, $\nu = \sqrt{\frac{\pi}{2}}a/w$, where a is the aperture radius and w_z is beam width . It's essential to understand that the evaluation in (10) is true for $w_z > 6\,a$. Consider r, follows the Nakagami-m distribution expressed as [16],

$$f_r\left(r\right) = \frac{2\,m^m\,r^{2m-1}}{\Omega^m\Gamma\left(m\right)}\exp\left(\frac{-m\,r^2}{\Omega}\right), \tag{11}$$

where, the shaping parameter $m \ge 0.5$ and scaling parameter $\Omega > 0$. Using equation (10) and (11), $f_{h_p}\left(h_p\right)$ is given by ,

$$f_{h_p}\left(h_p\right) = \frac{\left(\zeta^2\right)^m}{\Gamma\left(m\right)A_o^{\zeta^2}}\left(\ln\left(\frac{A_o}{h_p}\right)\right)^{m-1} h_p^{\zeta^2-1}. \tag{12}$$

where, $\zeta = \frac{w_{zeq}}{2\sigma_s}$ represents the beam radius, w_{zeq} to the jitter σ_s ratio [9]. Equation (12), can be approximated to different distributions i.e., for $m = 1$ it represents the jitter effect with Rayleigh distribution. Also, $m > 1$ it can evaluate the non-zero boresight error modelled as Rician distribution and for $m = 0.5$ it can be approximated to one-sided Gaussian distribution.

C. Combined Channel Statistical Model

The effect of atmospheric fading combined with PEs and other atmospheric attenuations is termed as combined channel fading. As a result, the FSO communication is affected by multiple sources of attenuation in this scenario. The combined channel statistics, h can be expressed as [12],

$$f_h(h) = \int_{h/A_o\, h_l}^{\infty} f_{h_a}(h_a)\; f_{h/h_a}\left(\frac{h}{h_a h_l}\right)\, dh_a, \tag{13}$$

where, $f_{h/h_a}\left(\frac{h}{h_a h_l}\right)$ is the conditional probability for a given turbulence state h_a, can be expressed as,

$$f_{h/h_a}\left(\frac{h}{h_a}\right) = \frac{1}{h_a h_l} f_{h_p}\left(\frac{h}{h_a h_l}\right). \tag{14}$$

Consider clear sky weather condition, the atmospheric attenuation $h_l = 1$, correspondingly equation (14) as

$$f_{h/h_a}\left(\frac{h}{h_a}\right) = \frac{1}{h_a} f_{h_p}\left(\frac{h}{h_a}\right), \tag{15}$$

where, $0 \le h \le A_o h_a$ and $f_{h_p}\left(\frac{h}{h_a}\right)$ is,

$$f_{h_p}\left(\frac{h}{h_a}\right) = \frac{\left(\zeta^2\right)^m\, h^{\zeta^2-1}}{\Gamma(m)\, A_o^{\zeta^2}} \left(\ln\left(\frac{A_o h_a}{h}\right)\right)^{m-1} \left(\frac{1}{h_a}\right)^{\zeta^2}. \tag{16}$$

Substituting (9) and (16) into (13),

$$f_h(h) = C_1 \int_{\frac{h}{A_o}}^{\infty} \left[\ln\left(\frac{h_a A_o}{h}\right)\right]^{m-1} h_a^{b-\zeta^2-1} \; G_{0,2}^{2,0}\left(\begin{matrix} - \\ \frac{\alpha_l-\beta_s}{2}, \frac{\beta_s-\alpha_l}{2} \end{matrix} \;\middle|\; \alpha_l\beta_s h_a\right) h_a, \tag{17}$$

where,

$$C_1 = \frac{\left(\zeta^2\right)^m (\alpha_l\beta_s)^b\, h^{\left(\zeta^2-1\right)}}{\Gamma(\alpha_l)\,\Gamma(\beta_s)\,\Gamma(m)\, A_o^{\zeta^2}}$$

$$f_h(h) = Q_o\, h^{b-1} \; G_{1,3}^{3,0}\left(\begin{matrix} -, \left(1+\zeta^2-b\right) \\ (1+\zeta^2-b-m), (\frac{\alpha_l-\beta_s}{2}, \frac{\beta_s-\alpha_l}{2}) \end{matrix} \;\middle|\; \alpha_l\beta_s \frac{h}{A_o}\right), \tag{18}$$

where,

$$Q_o = \frac{\left(\zeta^2\right)^m (\alpha_l\beta_s)^b}{\Gamma(\alpha_l)\,\Gamma(\beta_s)\, A_o^b}.$$

The next section deals with the analytical framework of deriving the average bit error rate.

III. Average Bit Error Rate

The average BER performance of FSO communication over the combined channel effect is evaluated . The conditional PDF of $f_h(h)$ defined by,

$$P_b = \int_0^{\infty} P_e\, f_h(h)\, dh, \tag{19}$$

where P_e represents the conditional probability expressed as [21],

$$P_e = Q\left(\sqrt{\frac{SNR}{2}}\right), \tag{20}$$

where, the instantaneous SNR can be represented as,

$$SNR = \frac{\overline{SNR}}{k^2\, A_o^2}\, h^2,$$

$$P_e = Q\left(\sqrt{\frac{\overline{SNR}}{2k^2\, A_o^2}\, h^2}\right), \tag{21}$$

where $Q(.)$ represents the Q function given as complementary error function $erfc(.)$ (where, $erfc(x) = 2Q\left(\sqrt{2}\,x\right)$) and expressing $erfc(x)$ by [20],

$$erfc(\sqrt{x}) = \frac{1}{\sqrt{\pi}}\, G_{1,2}^{2,0}\left[\begin{matrix} 1 \\ 0, \frac{1}{2} \end{matrix} \;\middle|\; x\right].$$

Equation (21) can be expressed as,

$$P_e = \frac{1}{2\sqrt{\pi}}\, G_{1,2}^{2,0}\left[\begin{matrix} 1 \\ 0, \frac{1}{2} \end{matrix} \;\middle|\; \frac{\overline{SNR}}{(2A_o k)^2}\, h^2\right]. \tag{22}$$

On substituting equation (18) and (22) in (19), can be expressed as,

$$P_b = \frac{Q_0}{2\sqrt{\pi}} \int_0^{\infty} h^{b-1}\, G_{1,2}^{2,0}\left[\begin{matrix} 1 \\ 0, \frac{1}{2} \end{matrix} \;\middle|\; \frac{\overline{SNR}}{(2A_o\, k)^2}\, h^2\right] G_{1,3}^{3,0}\left[\begin{matrix} 1+\zeta-b \\ 1+\zeta-b-m, \alpha_l-1, \beta_s-1 \end{matrix} \;\middle|\; \frac{\alpha_l\beta_s}{A_o}\, h\right] dh. \tag{23}$$

Average BER can be derived by using the approximation [20],

$$P_b = \frac{Q_0}{2\sqrt{\pi}} \times G_{7,4}^{2,6}\left[\begin{matrix} 1, \frac{m-\zeta}{2}, \frac{1+m-\zeta}{2}, \frac{1-\alpha_l}{2}, \frac{2-\alpha_l}{2}, \frac{1-\beta_s}{2}, \frac{2-\beta_s}{2}, \\ 0, \frac{1}{2}, \frac{-\zeta}{2}, \frac{1-\zeta}{2} \end{matrix} \;\middle|\; t\right] \tag{24}$$

where, $t = \frac{4\,\overline{SNR}}{(k\,\alpha_l\,\beta_s)^2}$.

The following section addresses the necessary experimental testbed for the performance evaluation.

IV. Experimental Set-up

To evaluate the performance of FSO communicators, an experimental testbed with a controlled atmospheric turbulence channel is developed. A detailed schematic diagram describing the experimental setup under indoor atmospheric turbulence conditions is shown in Fig. 1. An indoor atmospheric chamber with 2.5 m X 0.5 m X 0.5 m is designed with two heating elements one at each end perpendicular to the propagating beam. Two cooling fans are arranged at each end of the chamber to maintain temperature variations. Two temperature sensors at each end of the heating element record the chamber temperature [22]. A detailed FSO communication operating at 635 nm setup is designed in our previous work [23]. Atmospheric turbulence is generated by controlling the temperature of heating elements, where a temperature gradient creates beam wandering effect. The

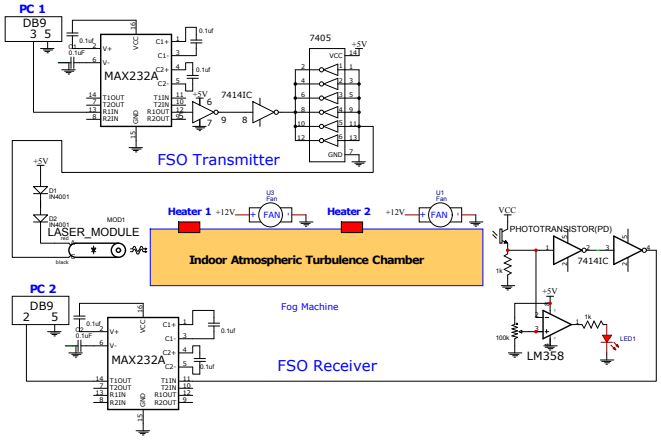

Fig. 1. Schematic of FSO communication under indoor atmospheric turbulence chamber

scintillation index determines the degree of turbulence caused due to variation in the temperature expressed as [24],

$$C_n^2 = \left(86 \times 10^{-6} \frac{P}{T^2}\right) C_T^2, \tag{25}$$

where, T, represents the absolute temperature (Kelvin), P represents the atmospheric pressure (milibar), and C_T^2 is the temperature function structure evaluated as [24]:

$$\begin{aligned} D_T &= \left\langle (T_1 - T_2)^2 \right\rangle \\ &= \begin{cases} C_T^2\, l_0^{-4/3} z^2, & for\ 0 \ll z \ll l_0 \\ C_T^2\, l_0^{2/3}, & for\ l_0 \ll z \ll L_0 \end{cases}, \end{aligned} \tag{26}$$

where, l_0, L_0 are the inner scale due to small eddies and the outer scale caused due to large eddies of the light caused by the changes in temperature. T_1 and T_2 represent the temperatures at two points which are located by the propagation link distance of z.

An image is transmitted in an atmospheric turbulence environment to analyze the effect of FSO communication across different turbulence strenghths [22]. Peak signal-to-noise ratio (PSNR) forms the parameter to measure the quality of received image. PSNR is given as [25],

$$PSNR = 20 \log \left(\frac{MPV^2}{\sqrt{MSE}}\right), \tag{27}$$

where, MPV signifies the maximum possible value of an image and MSE is the mean square error to measure the used to estimate the error associated with the received image comparing that with the transmitted image as [22],

$$MSE = \frac{1}{xy} \sum_{k=0}^{x-1} \sum_{l=0}^{y-1} \left[T_x\,(k,l) - R_x\,(k,l)\right]^2, \tag{28}$$

where, T_x and R_x are $x \times y$ monochromatic transmitted and received image respectively. The next section presents the results and discussion of the different factors affecting the system

V. Results and Discussion

FSO communication system's performance is numerically evaluated using MATLAB 2018a. Simulation parameters considered are the link range of 3.5 km, operating wavelength at 1550 nm, radius of aperture (a) of 0.1 m and jitter standard deviation (σ_s) as 1 m.

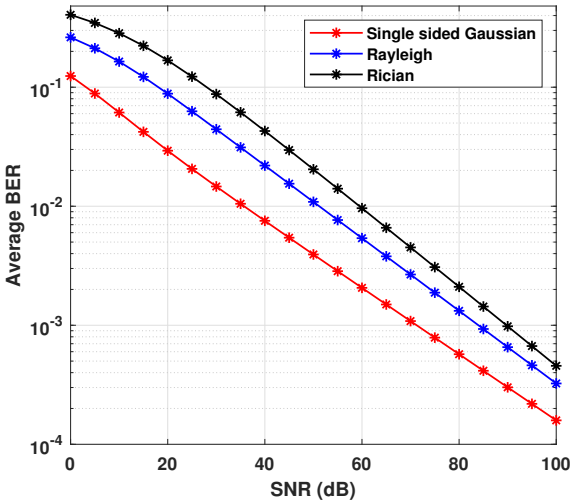

Fig. 2. Average BER for different PEs effect

Fig. 2, represents the BER performance of FSO communication evaluated under atmospheric turbulence (with $\alpha_l = 18$ and $\beta_s = 12$) for different PEs conditions. Different PEs scenarios considering jitter, and non-zero boresight error are taken into account with the appropriate special cases of radial distribution modelled accordingly. For $m = 1$ it represents the jitter effect with Rayleigh distribution. Also, $m > 1$ for the non-zero boresight error modelled as Rician distribution and for $m = 0.5$ as one-sided Gaussian distribution in equation (24). It can be observed that as the PEs dominate the system, BER has been considerably increased.

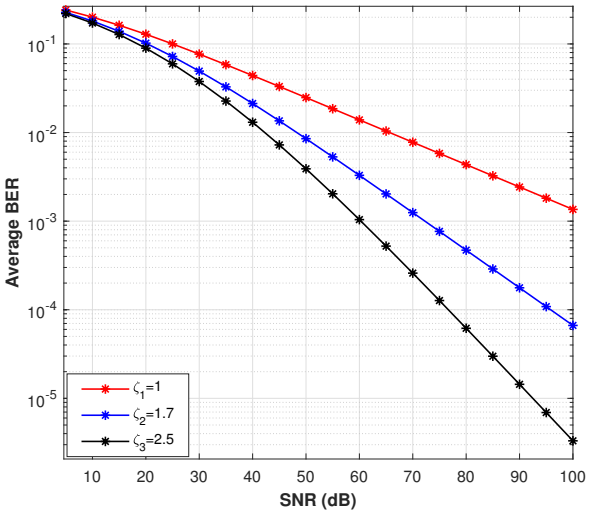

Fig. 3. Average BER for different beam radius to jitter ratio (ζ)

Fig. 3 represents the BER performance for different beamwidth values to jitter variance, ζ under moderate turbulence ($\alpha_l = 6$ and $\beta_s = 4$). BER decreased considerably as the beamwidth to jitter variance ratio increased. An increase in beamwidth, reduces the effect of PEs. A more significant increase in the beamwidth can reduce PEs, but decreases the received power and SNR resulting poor BER performance. A trade off between the beamwidth size for the required BER is to be optimized accordingly.

An atmospheric chamber is designed and analyzed the atmospheric turbulence using the corresponding testbed shown in Fig. 4. The chamber is precisely positioned to permit airflow through the laser's propagation route. The temperature of heater one and heater two are adjusted to produce the desired temperatures (T_1 and T_2), and corresponding turbulence strength is generated as shown in Table I. Atmospheric turbulence is characterized as weak, moderate and strong turbulence. For weak turbulence $C_n^2 \leq 10^{-15}$ and for moderate to strong turbulence $C_n^2 > 10^{-15}$ [25].

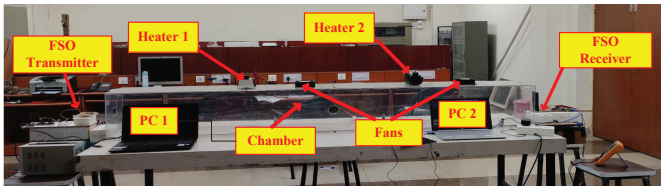

Fig. 4. Experimental setup of FSO communication under indoor atmospheric turbulence chamber.

TABLE I
EXPERIMENTAL MEASUREMENTS OF INDOOR ATMOSPHERIC TURBULENCE.

Sl. No	$T_1(K)$	$T_2(K)$	$C_n^2(m^{-2/3})$	Turbulence strength
1	304.75	302.55	2.60602E-12	Strong
2	302.35	302.15	4.99201E-13	Moderate
3	302.45	302.55	4.91981E-15	Weak

TABLE II
RECEIVED IMAGE UNDER DIFFERENT ATMOSPHERIC TURBULENCE SCENARIOS.

Sr. No.	Turbulence Strength	PSNR (dB)	Transmitted / Received Image
1	No turbulence	42.2	
2	Weak	35.64	
3	Moderate	22.4	
4	Strong	6.128	

A monochrome image is transmitted under different atmospheric turbulence conditions as shown in Table II. It is noticed that under the absence of turbulence, the received image has a high PSNR of 42.2 dB. The image quality is degraded due to the various strengths of atmospheric turbulence which causes fading like phenomenon of received power in FSO communication.

VI. CONCLUSION

FSO communication performance taking into the effect of atmospheric turbulence and generalized PEs are analyzed in this research work. A generalized analytical closed-form framework for average BER is derived over atmospheric turbulence and generalized PEs. An experimental evaluation by transmitting an image under different channel conditions provides deeper insights into the link performance under clear weather conditions. A more in depth analysis can be performed involving angle of arrival (AoA) associated due to beam wandering. An efficient tracking mechanism to overcome the link misalignment caused due to PE, AoA, atmospheric turbulence, and other atmospheric conditions can be designed.

REFERENCES

[1] D. J. Heatley, D. R. Wisely, I. Neild, and P. Cochrane, "Optical wireless: The story so far," *IEEE Communications Magazine*, vol. 36, no. 12, pp. 72–74, 1998.

[2] A. A. Farid and S. Hranilovic, "Outage capacity optimization for free-space optical links with pointing errors," *Journal of Lightwave Technology*, vol. 25, no. 7, pp. 1702–1710, 2007.

[3] S. H. Ali, "Advantages and limits of free space optics," *International Journal of Advanced Smart Sensor Network Systems (IJASSN)*, vol. 9, no. 1/2/3, 2019.

[4] S. Karp, R. Gagliardi, S. Moran, and L. Stotts, "Optical channels: Fiber, atmosphere, water and clouds," 1988.

[5] L. C. Andrews, R. L. Phillips, C. Y. Hopen, and M. Al-Habash, "Theory of optical scintillation," *JOSA A*, vol. 16, no. 6, pp. 1417–1429, 1999.

[6] A. Al-Habash, L. C. Andrews, and R. L. Phillips, "Mathematical model for the irradiance probability density function of a laser beam propagating through turbulent media," *Optical engineering*, vol. 40, no. 8, pp. 1554–1562, 2001.

[7] J. Barry and G. Mecherle, "Beam pointing error as a significant design parameter for satellite-borne, free-space optical communication systems," *Optical Engineering*, vol. 24, no. 6, p. 241049, 1985.

[8] P. Saxena, A. Mathur, M. R. Bhatnagar, and Z. Ghassemlooy, "BER of an optically pre-amplified FSO system under malaga turbulence, pointing errors, and ASE noise," in *Annual International Symposium on Personal, Indoor, and Mobile Radio Communications (PIMRC)*. IEEE, 2017, pp. 1–6.

[9] F. Yang, J. Cheng, and T. A. Tsiftsis, "Free-space optical communication with nonzero boresight pointing errors," *IEEE Transactions on Communications*, vol. 62, no. 2, pp. 713–725, 2014.

[10] H. G. Sandalidis, T. A. Tsiftsis, G. K. Karagiannidis, and M. Uysal, "BER performance of FSO links over strong atmospheric turbulence channels with pointing errors," *IEEE Communications Letters*, vol. 12, no. 1, pp. 44–46, 2008.

[11] P. Kaur, V. K. Jain, and S. Kar, "Performance analysis of FSO array receivers in presence of atmospheric turbulence," *IEEE Photonics Technology Letters*, vol. 26, no. 12, pp. 1165–1168, 2014.

[12] A. Touati, A. Abdaoui, F. Touati, M. Uysal, and A. Bouallegue, "On the effects of combined atmospheric fading and misalignment on the hybrid FSO/RF transmission," *Journal of Optical Communications and Networking*, vol. 8, no. 10, pp. 715–725, 2016.

[13] H. G. Sandalidis, T. A. Tsiftsis, and G. K. Karagiannidis, "Optical wireless communications with heterodyne detection over turbulence channels with pointing errors," *Journal of Lightwave Technology*, vol. 27, no. 20, pp. 4440–4445, 2009.

[14] W. Gappmair, S. Hranilovic, and E. Leitgeb, "OOK performance for terrestrial FSO links in turbulent atmosphere with pointing errors modeled by Hoyt distributions," *IEEE Communications Letters*, vol. 15, no. 8, pp. 875–877, 2011.

[15] H. Singh and A. S. Sappal, "Moment-based approach for statistical and simulative analysis of turbulent atmospheric channels in FSO communication," *IEEE Access*, vol. 7, pp. 11 296–11 317, 2019.

[16] V. K. Kappala, J. Pradhan, A. K. Turuk, V. N. Silva, S. Majhi, and S. K. Das, "A point-to-multi-point tracking system for FSO communication," *IEEE Transactions on Instrumentation and Measurement*, vol. 70, pp. 1–10, 2021.

[17] G. T. Djordjevic, M. I. Petkovic, M. Spasic, and D. S. Antic, "Outage capacity of FSO link with pointing errors and link blockage," *Optics express*, vol. 24, no. 1, pp. 219–230, 2016.
[18] D. H. Ai, H. D. Trung, and D. T. Tuan, "On the ASER performance of amplify-and-forward relaying MIMO/FSO systems using SC-QAM signals over log-normal and gamma-gamma atmospheric turbulence channels and pointing error impairments," *Journal of Information and Telecommunication*, vol. 4, no. 3, pp. 267–281, 2020.
[19] X. Tang, Z. Wang, Z. Xu, and Z. Ghassemlooy, "Multihop free-space optical communications over turbulence channels with pointing errors using heterodyne detection," *Journal of Lightwave Technology*, vol. 32, no. 15, pp. 2597–2604, 2014.
[20] Meijer-G function. [Online]. Available: https://functions.wolfram.com/HypergeometricFunctions/MeijerG/21/02/03/01/0002/MainEq1.L.gif
[21] W. Gappmair and M. Flohberger, "Error performance of coded FSO links in turbulent atmosphere modeled by gamma-gamma distributions," *IEEE Transactions on Wireless Communications*, vol. 8, no. 5, pp. 2209–2213, 2009.
[22] A. Aldaihan, M. Ijaz, S. Ekpo, A. Gibson, Z. Ghassemlooy, K. Rabie, and B. Adebisi, "Experimental results on the mitigation of turbulence in free space optics using spatial diversity," in *International Symposium on Communication Systems, Networks and Digital Signal Processing (CSNDSP)*. IEEE, 2020, pp. 1–5.
[23] K. V. Kiran, S. Rathore, A. K. Turuk, and S. K. Das, "Development of a hybrid FSO/RF system during link misalignment," in *International Conference on Networking and Network Applications (NaNA)*. IEEE, 2017, pp. 138–140.
[24] L. C. Andrews and R. L. Phillips, "Laser beam propagation through random media." SPIE, 2005.
[25] Z. Ghassemlooy, W. Popoola, and S. Rajbhandari, *Optical wireless communications: system and channel modelling with Matlab®*. CRC press, 2019.